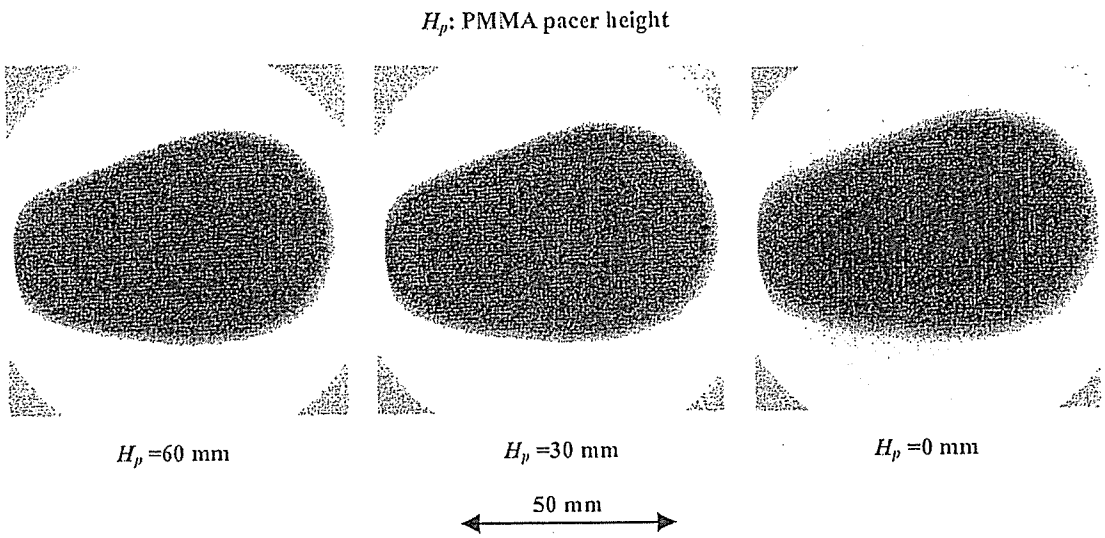

Fig. 8. Radiograms of a polycapillary plate according to changes in the PMMA height.

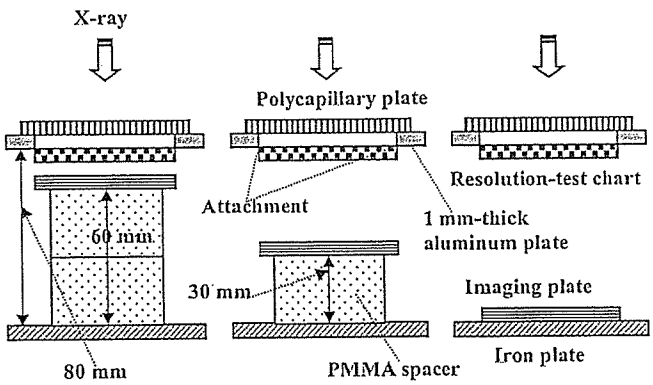

Fig. 9. Radiography for imaging a test chart using a polycapillary plate.

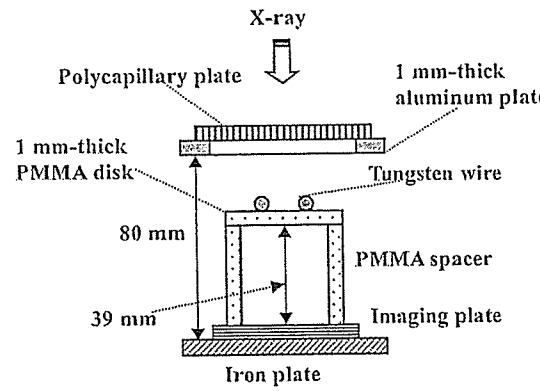

Fig. 11. Radiography for imaging tungsten wires using the polycapillary.

Fig. 9 shows the parallel radiography for imaging a test chart, and the polycapillary was placed on the aluminum plate. In this radiography, when the spacer height was increased, we observed 100 μm lines, and the image dimensions decreased slightly (Fig. 10).

Figs. 11 and 12 show radiography and the radiogram of tungsten wires on a PMMA spacer, respectively. Although the image contrast increased with increases in the wire diameter, a 50 μm-diameter wire could be observed. An angiography of a rabbit heart is shown in Fig. 13; iodine-based

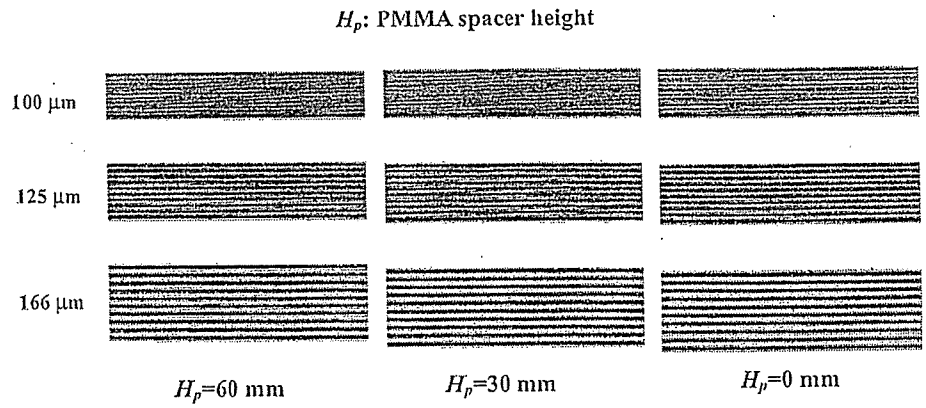

Fig. 10. Radiograms of a test chart using the polycapillary according to changes in the height.

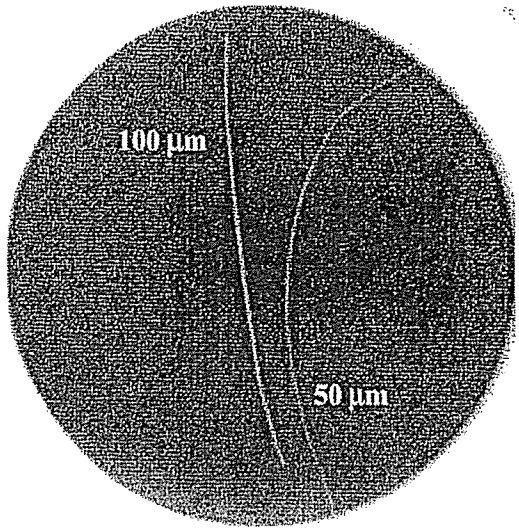

Fig. 12. Radiograms of tungsten wires on a PMMA spacer.

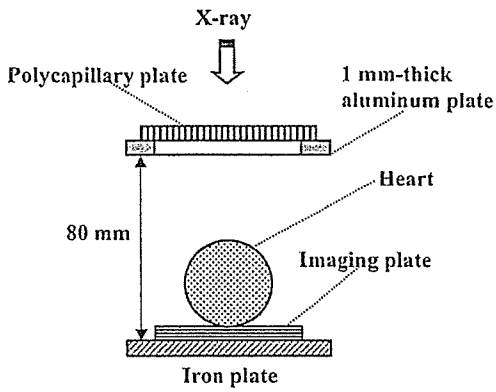

Fig. 13. Parallel angiography of a heart extracted from a rabbit using iodine-based microspheres.

microspheres of 15 μm-diameter were used, and fine blood vessels of about 100 μm were clearly visible (Fig. 14).

5. Discussion

Using this polycapillary plate, we performed a quasi-monochromatic parallel radiography system using a polycapillary plate in conjunction with a CR system.

If we assume that the incident angle for reflection in the capillary hole is constant, the X-ray intensity without absorbing I_0, the transmission intensity I_t, the reflecting intensity I_r, and the intensity for parallel radiography I may be given by (Fig. 15):

$$I_0 = K_1 \sum_{i=1}^{n} I_k(E_i) \exp\{-\mu(E_i)a\}, \quad (1)$$

$$I_t \cong K_2 \sum_{i=1}^{n} I_k(E_i) \exp\{-\mu(E_i)a - \mu_c(E_i)b\}, \quad (2)$$

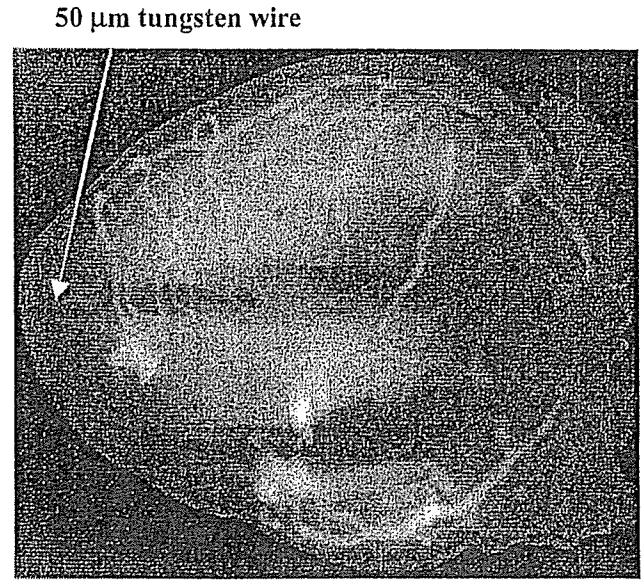

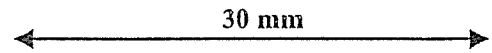

Fig. 14. Angiogram of the heart using the polycapillary.

$$I_r \cong K_3 \sum_{i=1}^{n} I_k(E_i) \exp\{-\mu(E_i)a\} \cdot R(E_i)^m, \quad (3)$$

$$I \cong I_0 + I_r \gg I_t, \quad (4)$$

where $I_k(E_i)$ is the ith characteristic X-ray intensity from the tube, $\mu(E_i)$ the linear absorption coefficient of copper filter, $\mu_c(E_i)$ is the linear absorption coefficient of capillary glass, $R(E_i)$ is the reflecting power ($1 \geqq R(E_i) \geqq 0$), m is the number of reflection, n is the number of characteristic X-rays, a is the filter thickness, b is capillary thickness, and K_1–K_3 are constants.

In this research, we performed parallel radiography achieved with a polycapillary plate in conjunction with quasi-monochromatic X-rays, and higher image resolutions as compared with those obtained without using the plate were obtained. Currently, because the resolution improves

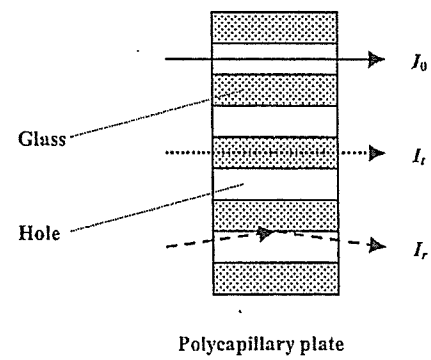

Fig. 15. Characteristic X-ray transmissions in the polycapillary plate. In the parallel radiography, the radiographic object is taken by both the direct transmission rays through capillaries I_0 and the reflection rays on the insides of holes I_r.

with corresponding decreases in the hole diameter of the capillary, this system can be applied to image a wide variety of objects in various fields including medical radiography.

6. Summary

In summary, we developed a conventional quasi-monochromatic parallel radiography system utilizing a polycapillary plate with a hole diameter of 25 μm and a CR system. Quasi-monochromatic characteristic X-rays were obtained by a 10 μm-thick copper filter with a tube voltage of 20 kV. The X-rays from the tube were formed into parallel beams in order to perform radiography. The image dimension increased slightly with corresponding increases in the distance between the radiographic object and the imaging plate, and we observed a 50 μm tungsten wire and fine blood vessels clearly.

Acknowledgements

This work was supported by Grants-in-Aid for Scientific Research and Advanced Medical Scientific Research from MECSST (12670902, 13470154, and 13877114), Grants from Keiryo Research Foundation, JST (Test of Fostering Potential), NEDO, and MHLW (HLSRG, RAMT-nano-001, RHGTEFB-genome-005, and RGCD13C-1).

References

[1] E. Sato, S. Kimura, S. Kawasaki, H. Isobe, K. Takahashi, Y. Tamakawa, T. Yanagisawa, Rev. Sci. Instrum. 61 (1990) 2343.
[2] E. Sato, A. Shikoda, S. Kimura, M. Sagae, T. Oizumi, K. Takahashi, Y. Hayasi, T. Shoji, K. Shishido, Y. Tamakawa, T. Yanagisawa, SPIE 1801 (1992) 628.
[3] E. Sato, M. Sagae, K. Takahashi, T. Oizumi, H. Ojima, K. Takayama, Y. Tamakawa, T. Yanagisawa, A. Fujiwara, K. Mitoya, SPIE 2513 (1994) 649.
[4] E. Sato, M. Sagae, K. Takahashi, A. Shikoda, T. Oizumi, H. Ojima, K. Takayama, Y. Tamakawa, T. Yanagisawa, A. Fujiwara, K. Mitoya, SPIE 2513 (1994) 723.
[5] A. Shikoda, E. Sato, M. Sagae, T. Oizumi, Y. Tamakawa, T. Yanagisawa, Rev. Sci. Instrum. 65 (1994) 850.
[6] E. Sato, K. Takahashi, M. Sagae, S. Kimura, T. Oizumi, Y. Hayasi, Y. Tamakawa, T. Yanagisawa, Med. Biol. Eng. Comput. 32 (1994) 289.
[7] K. Takahashi, E. Sato, M. Sagae, T. Oizumi, Y. Tamakawa, T. Yanagisawa, Jpn. J. Appl. Phys. 33 (1994) 4146.
[8] E. Sato, M. Sagae, A. Shikoda, K. Takahashi, T. Oizumi, M. Yamamoto, A. Takabe, K. Sakamaki, Y. Hayasi, H. Ojima, K. Takayama, Y. Tamakawa, SPIE 2869 (1996) 937.
[9] E. Sato, R. Germer, Y. Hayasi, E. Tanaka, H. Mori, T. Kawai, T. Usuki, K. Sato, H. Obara, M. Zuguchi, T. Ichimaru, H. Ojima, K. Takayama, H. Ido, SPIE 4948 (2002) 604.
[10] E. Sato, Y. Hayasi, R. Germer, E. Tanaka, H. Mori, T. Kawai, H. Obara, T. Ichimaru, K. Takayama, H. Ido, Jpn. J. Med. Imag. Inform. Sci. 20 (2003) 148.
[11] E. Sato, Y. Hayasi, R. Germer, E. Tanaka, H. Mori, T. Kawai, H. Obara, T. Ichimaru, K. Takayama, H. Ido, Jpn. J. Med. Phys. 20 (2003) 123.
[12] H. Mori, K. Hyodo, E. Tanaka, M.U. Mohammed, A. Yamakawa, Y. Shinozaki, H. Nakazawa, Y. Tanaka, T. Sekka, Y. Iwata, S. Honda, K. Umetani, H. Ueki, T. Yokoyama, K. Tanioka, M. Kubota, H. Hosaka, N. Ishizawa, M. Ando, Radiology 201 (1996) 173.
[13] T.J. Davis, D. Gao, T.E. Gureyev, A.W. Stevenson, S.W. Wilkims, Nature 373 (1995) 595.
[14] A. Momose, T. Takeda, Y. Itai, K. Hirano, Nat. Med. 2 (4) (1996) 473.
[15] A. Ishisaka, H. Ohara, C. Honda, Opt. Rev. 7 (2000) 566.
[16] A.A. Bzhanmikov, N. Langhoff, J. Schmalz, R. Wedell, V.L. Beloglazov, N.F. Lebedev, SPIE 3444 (1998) 430.
[17] Q.F. Xiao, S.V. Poturaef, Nucl. Instr. Meth. Phys. Res. A 347 (1994) 376.
[18] E. Sato, Y. Hayasi, E. Tanaka, H. Mori, T. Kawai, H. Obara, T. Ichimaru, K. Takayama, H. Ido, T. Usuki, K. Sato, Y. Tamakawa, SPIE 4508 (2001) 176.
[19] E. Sato, H. Toriyabe, Y. Hayasi, E. Tanaka, H. Mori, T. Kawai, T. Usuki, K. Sato, H. Obara, T. Ichimaru, K. Takayama, H. Ido, Y. Tamakawa, SPIE 4682 (2002) 298.
[20] E. Sato, Y. Hayasi, T. Usuki, K. Sato, H. Ojima, K. Takayama, H. Ido, in: Proceedings of the 3rd Korea-Japan Joint Meeting on Medical Physics, Gyeongju, 2002, p. 400.
[21] E. Sato, K. Sato, Y. Tamakawa, Ann. Rep. Iwate Med. Univ. Sch. Lib. Arts Sci. 35 (2000) 13.

Available online at www.sciencedirect.com
SCIENCE DIRECT®
Journal of Electron Spectroscopy and Related Phenomena 137–140 (2004) 699–704
JOURNAL OF ELECTRON SPECTROSCOPY and Related Phenomena
www.elsevier.com/locate/elspec

Portable X-ray generator utilizing a cerium-target radiation tube for angiography

E. Sato [a,*], Y. Hayasi [a], R. Germer [b], E. Tanaka [c], H. Mori [d], T. Kawai [e], T. Ichimaru [f], S. Sato [g], K. Takayama [h], H. Ido [i]

[a] *Department of Physics, Iwate Medical University, Morioka 020-0015, Japan*
[b] *ITP, FHTW FB1 and TU-Berlin, D 12249 Berlin, Germany*
[c] *Department of Nutritional Science, Faculty of Applied Bio-science, Tokyo University of Agriculture, Setagayaku 156-8502, Japan*
[d] *Department of Cardiac Physiology, National Cardiovascular Center Research Institute, Osaka 565-8565, Japan*
[e] *Electron Tube Division #2, Hamamatsu Photonics Inc., Iwata-gun 438-0193, Japan*
[f] *Department of Radiological Technology, School of Health Sciences, Hirosaki University, Hirosaki 036-8564, Japan*
[g] *Department of Microbiology, School of Medicine, Iwate Medical University, Morioka 020-8505, Japan*
[h] *Shock Wave Research Center, Institute of Fluid Science, Tohoku University, Sendai 980-8577, Japan*
[i] *Department of Applied Physics and Informatics, Faculty of Engineering, Tohoku Gakuin University, Tagajo 985-8537, Japan*

Available online 15 April 2004

Abstract

The development of a portable X-ray generator with a cerium-target tube and its application to angiography are described. The portable X-ray generator consists of a main controller, a unit with a Cock–Croft circuit and an X-ray tube, and a personal computer. Negative high voltages are applied to the cathode electrode in the X-ray tube, and the tube voltage and current are regulated by the controller or the computer. The X-ray tube is a glass-enclosed double-focus diode with a cerium target and a 0.5 mm-thick beryllium window. The maximum tube voltage and current were 60 kV and 0.8 mA, respectively. The focal-spot sizes were 4 mm × 4 mm (large) and 1 mm × 1 mm (small), respectively. Angiography was performed with a computed radiography system using iodine-based microspheres. The tube voltage, the current, the distance between the imaging plate and the X-ray source, and the spot size were 60 kV, 0.4 mA, 1.5 m, and small, respectively. In this angiography, we observed coronary arteries and fine blood vessels of about 50 μm or less with high contrasts.

Keywords: Cerium-target X-ray tube; Cerium characteristic X-rays; K-absorption edge; High contrast angiography; Microangiogrphy

1. Introduction

In conjunction with single crystals, synchrotrons generate monochromatic X-rays. These rays play an important role in parallel radiography and have been employed to perform high-contrast micro-angiography [1] and phase imaging [2–4]. However, it is difficult to obtain sufficient machine times for various research projects including medical applications.

So far, several different flash X-ray generators have been developed [5,6], and soft generators [7–12] with photon energies of lower than 150 keV can be employed to perform biomedical radiography. In order to produce monochromatic X-rays, plasma flash X-ray generators [13–16] are useful, since quite intense and sharp characteristic X-rays such as lasers have been produced from weakly ionized linear plasmas of nickel, copper and molybdenum, while bremsstrahlung rays are hardly detected at all. Using these generators, the characteristic X-ray intensity substantially increased with corresponding increases in the charging voltage.

Since K-series characteristic X-rays from cerium target are absorbed effectively by iodine-based contrast mediums, a cerium-target X-ray tube is very useful in order to perform high-contrast angiography. On the other hand, cerium is a rare earth element and has a high reactivity, and it is difficult to design the target. However, the development of a cerium-target tube for high-contrast angiography has long been wished for.

* Corresponding author.
E-mail address: dresato@iwate-med.ac.jp (E. Sato).

0368-2048/$ – see front matter © 2004 Elsevier B.V. All rights reserved.
doi:10.1016/j.elspec.2004.02.011

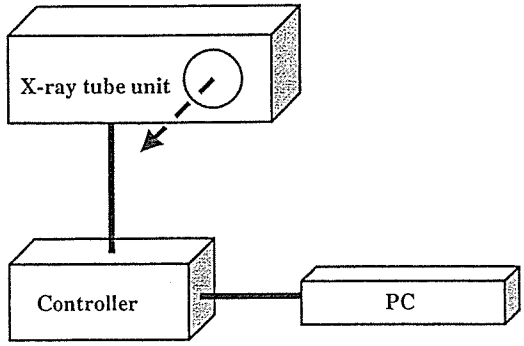

Fig. 1. Block diagram of the portable X-ray generator with a cerium-target radiation tube, which is specially used for angiography using iodine-based contrast mediums. The negative high voltage is applied to the cathode electrode, and the tube current is regulated by the filament temperature. Although the X-ray tube is a double-focus type, we usually employ a small focus in order to measure the radiographic characteristics and to perform angiography.

In the present research, we developed a portable X-ray generator with a cerium-target tube, used to perform preliminary study on angiography achieved with cerium K-series characteristic X-rays.

2. Generator

Fig. 1 shows the block diagram of the X-ray generator, which consists of a main controller, an X-ray tube unit with a Cockcroft circuit and a cerium-target tube, and a personal computer. The negative high-voltage is applied to the cathode electrode, and the anode (target) is connected to the ground potential. In this experiment, the tube voltage was regulated from 40 to 65 kV, and the tube current was regulated within 0.8 mA by the filament temperature. The exposure time is controlled in order to obtain optimum X-ray intensity, and the X-ray tube is a double-focus type with focal-spot dimensions of approximately 4 mm × 4 mm (large spot) and 1 mm × 1 mm (small spot), respectively. The maximum tube current is determined by the spot dimensions, and the currents of small and large spots are 0.4 and 0.8 mA, respectively.

3. Characteristics

3.1. X-ray intensity

X-ray intensity was measured by a Victoreen 660 ionization chamber at 1.0 m from the X-ray source using a small spot with an exposure time of 1.0 s (Fig. 2). At a constant tube current of 40 μA, the X-ray intensity increased when the tube voltage was increased. The intensity was roughly in proportion to the tube current at a constant tube voltage of 60 kV. In this measurement, the intensity with a tube voltage of 60 kV and a current of 90 μA was 2.14 μC/kg at 1.0 m from the source with errors of less than 0.2%.

3.2. X-ray source

In order to measure images of the X-ray source, we employed a pinhole camera with a hole diameter of 50 μm in conjunction with a computed radiography (CR) system (Fig. 3) [17]. When the tube voltage was increased, the spot intensity increased slightly, and spot dimensions seldom varied and had values of approximately 1 mm × 1 mm.

3.3. X-ray spectra

In order to measure X-ray spectra, we employed a cadmium tellurium detector (CDTE2020X, Hamamatsu Photonics Inc.) (Fig. 4). Compared with a germanium detector, this detector has lower energy resolutions. When the tube voltage was increased, both the characteristic X-ray intensity and the maximum photon energy of bremsstrahlung X-rays increased. According to insertion of a monochromatic cerium oxide filter, quasi-monochromatic X-rays were obtained.

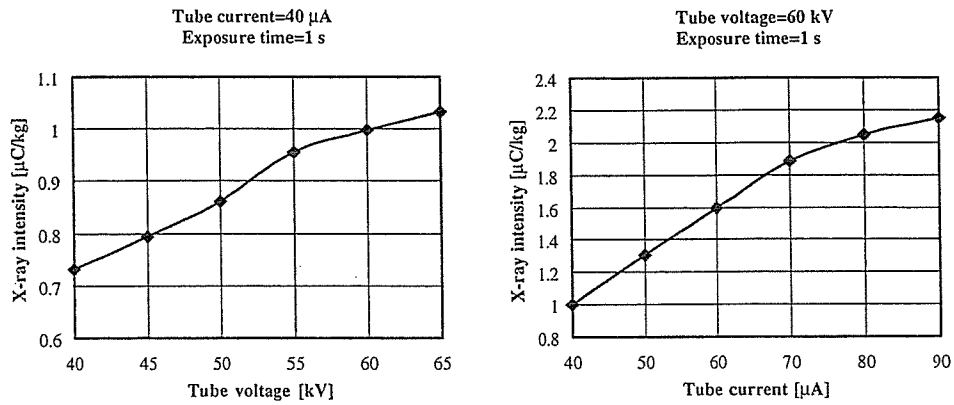

Fig. 2. X-ray intensity measured at 1.0 m from the X-ray source according to changes in the tube voltage and current. In the measurement, we employed an ionization chamber without using a monochromatic filter.

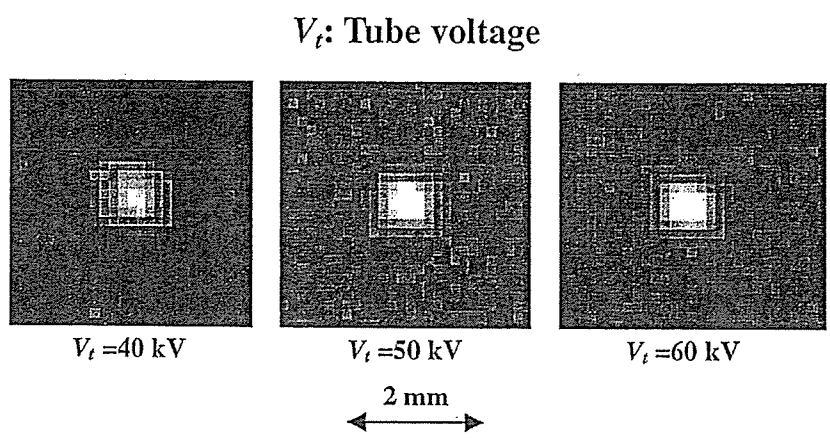

Fig. 3. Images of the X-ray source measured by a 100 mm diameter pinhole with changes in the tube voltage.

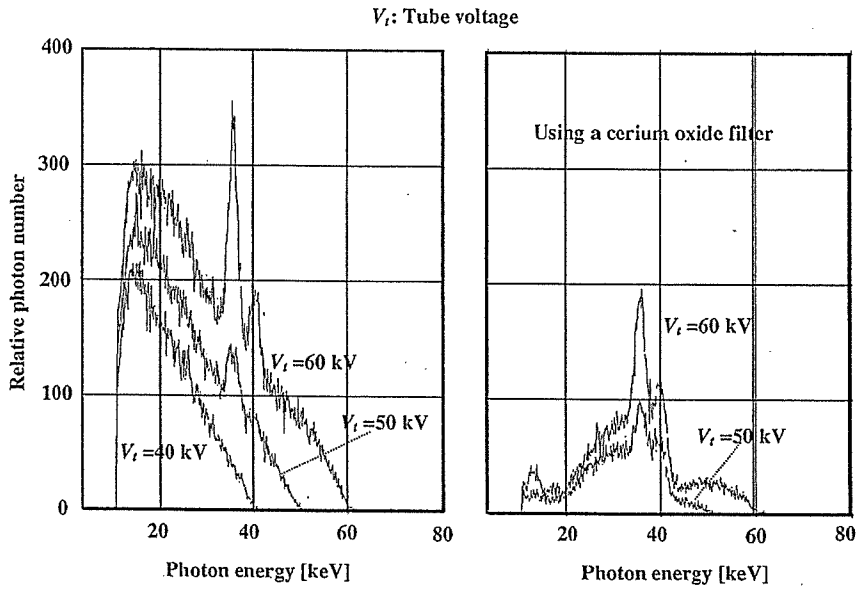

Fig. 4. X-ray spectra measured by a cadmium tellurium detector with changes in the tube voltage.

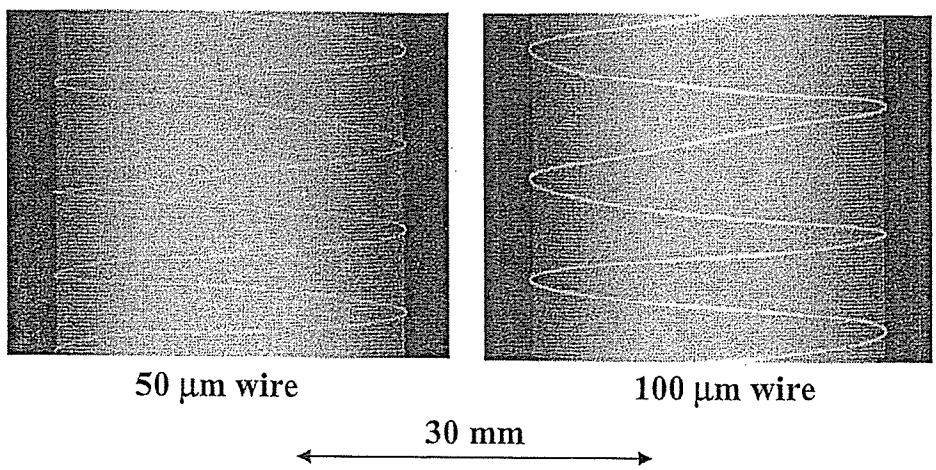

Fig. 5. Radiograms of tungsten wires around a rod made of PMMA used for estimating the image resolution.

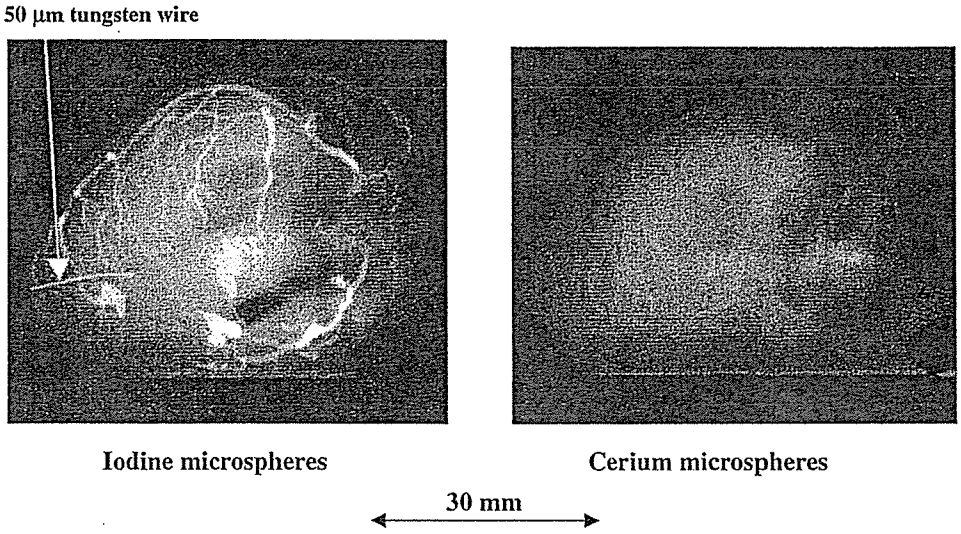

Fig. 6. Angiograms of rabbit hearts using (a) iodine and (b) cerium microspheres.

4. Angiography

The angiography was performed by a CR system (Konica Regius 150) using the monochromatic filter, and the distance (between the X-ray source and the imaging plate) and the tube voltage were 1.5 m and 60 kV, respectively.

Firstly, rough measurements of image resolution were made using wires. Fig. 5 shows radiograms of tungsten wires coiled around rods made of polymethyl methacrylate (PMMA). Although the image contrast increased with increases in the wire diameter, a 50 μm diameter wire could be observed.

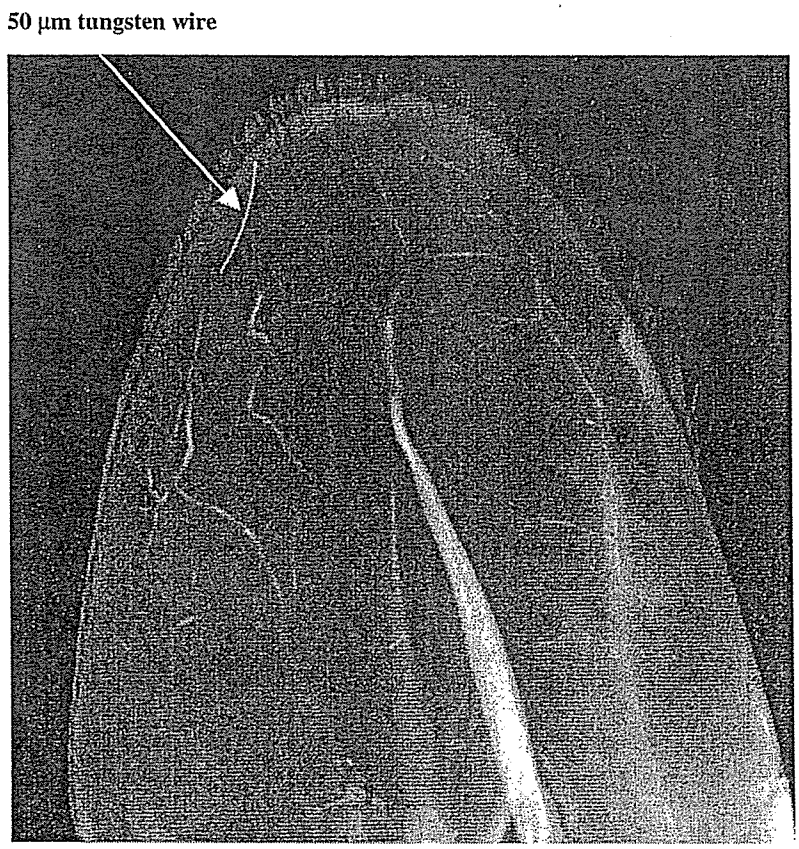

Fig. 7. Angiograms of the external ear of a rabbit using iodine-based microspheres. In this angiography, we employed a 50 μm tungsten wire to roughly determine the diameters of blood vessels.

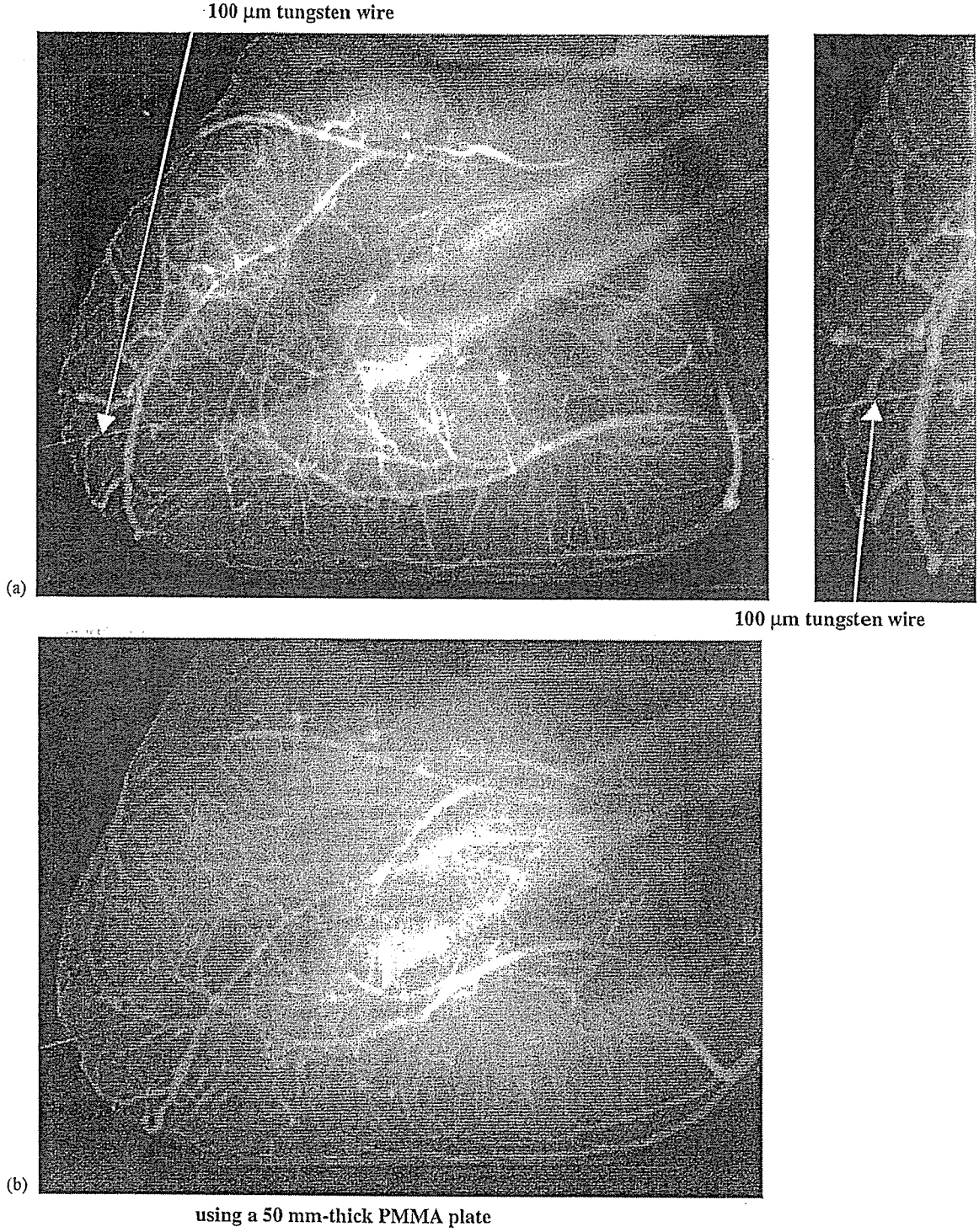

Fig. 8. Angiograms of an extracted heart of a dog. (a) Normal image and (b) image using a 50 mm PMMA plate set in front of the heart, facing the X-ray source.

Angiograms of rabbit hearts are shown in Fig. 6. These two images were obtained using iodine and cerium microspheres of 15 μm in diameter. In case where the cerium spheres were employed, the coronary arteries were barely visible. Fig. 7 shows an angiogram of the external ear of a rabbit using iodine spheres, and fine blood vessels of about 50 μm are clearly visible. In angiography of a larger heart extracted from a dog, using iodine spheres, a 50 mm thick PMMA plate was set in front of the heart facing X-ray source, and image contrast of coronary arteries decreased slightly with increases in the plate thickness (Fig. 8).

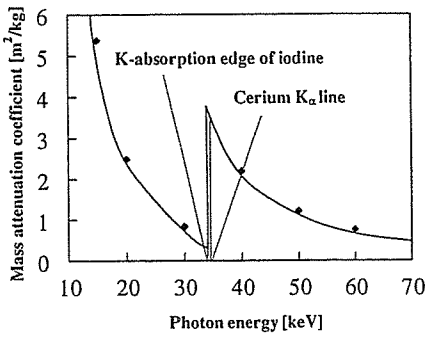

Fig. 9. Relation between the mass absorption coefficient of iodine and the photon energy of cerium Kα line.

5. Discussion

Cerium is a rare earth element and has a high reactivity. However, the average photon energy of Kα lines is 34.566 keV, and iodine spheres with a K-absorption edge of 33.155 keV absorb the lines easily (Fig. 9). Next, since the spheres easily transmit bremsstrahlung X-rays with energies of lower than the edge, it is important that the rays be absorbed as much as possible before angiography in order to increase the image contrast.

In rough measurement of image resolution, we obtained resolutions of 50 μm or less, and high-contrast blood vessels could be observed using a CR system. Although neogenetic fine blood vessels in recovery can be observed, the image resolution of the CR system should be improved as much as possible, and a dynamic CR system such as a flat panel system is useful to observe blood flows.

In this research, we developed a low-dose-rate X-ray tube in order to perform preliminary study on angiography using iodine-based contrast mediums. Because we are designing a high-dose-rate tube to decrease the exposure time, the K-series characteristic X-rays from cerium target can be employed to perform angiography for cases of cardiovascular disease.

6. Summary

In summary, we developed, new portable X-ray generator with a cerium-target tube and succeeded in producing K-series characteristic X-rays of cerium, which can be absorbed easily by iodine-based contrast mediums. Both the characteristic and bremsstrahlung X-ray intensities increased with corresponding increases in the tube voltage, and quasi-monochromatic X-rays were produced by a cerium oxide filter. In this preliminary experiment, although the maximum tube voltage and current were 65 kV and 0.4 mA, respectively, the voltage and current could be increased. Subsequently, we observed a 50 μm tungsten wire easily, and high-contrast angiography was performed using a CR system with an imaging plate.

Acknowledgements

This work was supported by Grants-in-Aid for Scientific Research and Advanced Medical Scientific Research from MECSST (12670902, 13470154, and 13877114), Grants from Keiryo Research Foundation, JST (Test of Fostering Potential), NEDO, and MHLW (HLSRG, RAMT-nano-001, RHGTEFB-genome-005, and RGCD13C-1).

References

[1] H. Mori, K. Hyodo, E. Tanaka, M.U. Mohammed, A. Yamakawa, Y. Shinozaki, H. Nakazawa, Y. Tanaka, T. Sekka, Y. Iwata, S. Honda, K. Umetani, H. Ueki, T. Yokoyama, K. Tanioka, M. Kubota, H. Hosaka, N. Ishizawa, M. Ando, Radiology 201 (1996) 173.
[2] T.J. Davis, D. Gao, T.E. Gureyev, A.W. Stevenson, S.W. Wilkims, Nature 373 (1995) 595.
[3] A. Momose, T. Takeda, Y. Itai, K. Hirano, Nature Med. 2 (4) (1996) 473.
[4] A. Ishisaka, H. Ohara, C. Honda, Opt. Rev. 7 (2000) 566.
[5] A. Mattsson, Phys. Scripta 5 (1972) 99.
[6] R. Germer, J. Phys. E Sci. Instrum. 12 (1979) 336.
[7] E. Sato, S. Kimura, S. Kawasaki, H. Isobe, K. Takahashi, Y. Tamakawa, T. Yanagisawa, Rev. Sci. Instrum. 61 (1990) 2343.
[8] E. Sato, M. Sagae, K. Takahashi, A. Shikoda, T. Oizumi, H. Ojima, K. Takayama, Y. Tamakawa, T. Yanagisawa, A. Fujiwara, K. Mitoya, SPIE 2513 (1994) 723.
[9] A. Shikoda, E. Sato, M. Sagae, T. Oizumi, Y. Tamakawa, T. Yanagisawa, Rev. Sci. Instrum. 65 (1994) 850.
[10] E. Sato, K. Takahashi, M. Sagae, S. Kimura, T. Oizumi, Y. Hayasi, Y. Tamakawa, T. Yanagisawa, Med. Biol. Eng. Comput. 32 (1994) 289.
[11] K. Takahashi, E. Sato, M. Sagae, T. Oizumi, Y. Tamakawa, T. Yanagisawa, Jpn. J. Appl. Phys. 33 (1994) 4146.
[12] E. Sato, M. Sagae, A. Shikoda, K. Takahashi, T. Oizumi, M. Yamamoto, A. Takabe, K. Sakamaki, Y. Hayasi, H. Ojima, K. Takayama, Y. Tamakawa, SPIE 2869 (1996) 937.
[13] E. Sato, Y. Hayasi, E. Tanaka, H. Mori, T. Kawai, T. Usuki, K. Sato, H. Obara, T. Ichimaru, K. Takayama, H. Ido, Y. Tamakawa, SPIE 4682 (2002) 538.
[14] E. Sato, R. Germer, Y. Hayasi, E. Tanaka, H. Mori, T. Kawai, T. Usuki, K. Sato, H. Obara, M. Zuguchi, T. Ichimaru, H. Ojima, K. Takayama, H. Ido, SPIE 4948 (2002) 604.
[15] E. Sato, Y. Hayasi, R. Germer, E. Tanaka, H. Mori, T. Kawai, H. Obara, T. Ichimaru, K. Takayama, H. Ido, Jpn. J. Med. Imag. Inform. Sci. 20 (2003) 148.
[16] E. Sato, Y. Hayasi, R. Germer, E. Tanaka, H. Mori, T. Kawai, H. Obara, T. Ichimaru, K. Takayama, H. Ido, Jpn. J. Med. Phys. 20 (2003) 123.
[17] E. Sato, K. Sato, Y. Tamakawa, Ann. Rep. Iwate Med. Univ. Sch. Lib. Arts Sci. 35 (2000) 13.

Quasi-monochromatic polycapillary imaging utilizing a computed radiography system

Eiichi Sato[a], Yasuomi Hayasi[a], Etsuro Tanaka[b], Hidezo Mori[c], Toshiaki Kawai[d], Toshio Ichimaru[e], Fumiko Obata[f], Kiyomi Takahashi[f], Sigehiro Sato[f], Kazuyoshi Takayama[g] and Hideaki Ido[h]

[a]Department of Physics, Iwate Medical University, 3-16-1 Honchodori, Morioka 020-0015, Japan
[b] Department of Nutritional Science, Faculty of Applied Bio-science, Tokyo University of Agriculture, 1-1-1 Sakuragaoka, Setagaya-ku 156-8502, Japan
[c] Department of Cardiac Physiology, National Cardiovascular Center Research Institute, 5-7-1 Fujishiro-dai, Suita, Osaka 565-8565, Japan
[d] Electron Tube Division #2, Hamamatsu Photonics Inc., 314-5 Shimokanzo, Toyooka Village, Iwata-gun 438-0193, Japan
[e] Department of Radiological Technology, School of Health Sciences, Hirosaki University, 66-1 Honcho, Hirosaki 036-8564, Japan
[f]Department of Microbiology, School of Medicine, Iwate Medical University, 19-1 Uchimaru, Morioka 020-8505, Japan
[g] Shock Wave Research Center, Institute of Fluid Science, Tohoku University, 2-1-1 Katahira, Aoba-ku, Sendai 980-8577, Japan
[h] Department of Applied Physics, Faculty of Engineering, Tohoku Gakuin University, 1-13-1 Chuo, Tagajo 985-8537, Japan

ABSTRACT

A fundamental study on quasi-monochromatic parallel radiography using a polycapillary plate and a copper-target x-ray tube is described. The x-ray generator consists of a negative high-voltage power supply, a filament (hot cathode) power supply, and an x-ray tube. The negative high-voltage is applied to the cathode electrode, and the anode electrode is connected to the ground. In this experiment, the tube voltage was regulated from12 to 22 kV, and the tube current was regulated within 3.0 mA by the filament temperature. The exposure time was controlled in order to obtain optimum x-ray intensity, and the maximum focal spot dimensions were approximately 2.0×1.5 mm. The polycapillary plate was J5022-16 (Hamamatsu Photonics Inc.), and the plate thickness was 1.0 mm. The outer, effective, and hole diameters were 33 mm, 27 mm, and 10 μm, respectively. Quasi-monochromatic x-rays were produced using a 10 μm-thick copper filter with a tube voltage of 17 kV, and these rays were formed into parallel beams by the polycapillary. The radiogram was taken using a computed radiography system utilizing imaging plates. In the measurement of image resolution, the resolution hardly varied according to increases in the distance between the chart and imaging plate using a polycapillary. We could observe a 50 μm tungsten wire clearly, and fine blood vessels of approximately 100 μm were visible in angiography.

Keywords: Parallel radiography, quasi-monochromatic x-ray, characteristic x-ray, x-ray lens, polycapillary plate

Laser-Generated & Other Lab. X-Ray & EUV Sources, Optics, Apps., ed. G. A. Kyrala, J.-C. J. Gauthier, C. A. MacDonald, A. M. Khounsary, Proceedings of SPIE Vol. 5196 (SPIE, Bellingham, WA, 2004) · 0277-786X/04/$15 · doi: 10.1117/12.505433

1. INTRODUCTION

Monochromatic parallel x-ray beams are typically produced by a synchrotron in conjunction with single crystals and have been applied in high contrast micro-angiography[1] and x-ray phase imaging.[2-4] In order to produce quasi-monochromatic x-rays without using the synchrotron, we developed a transmission type molybdenum x-ray tube.[5] Subsequently, flash x-ray tubes are employed to primarily perform high speed radiographies with biomedical applications. In particular, plasma flash x-ray tubes are very useful to produce intense and sharp characteristic x-rays[6-11] such as lasers.

With recent advances in x-ray optics, several different x-ray lenses[12,13] have been developed, and a polycapillary plate[5,8,14] has been shown to be useful to realize a low-priced x-ray system and to perform parallel radiography. Therefore, we performed parallel radiography using a tungsten-target x-ray tube and an x-ray film because the film is conventional and is useful to obtain a high image resolution.

In biomedical radiography, because both the brightness and the contrast of radiograms can be controlled by a Computed Radiography (CR) system[15] utilizing imaging plates, the CR system is useful to perform quasi-monochromatic parallel radiography, regardless of whether the image resolution falls. Therefore, in conjunction with the CR, we have to measure the fundamental characteristics of the polycapillary radiography.

In this paper, we describe a quasi-monochromatic parallel radiography system utilizing a fine polycapillary plate with a hole diameter of 10 μm, a CR system, and a copper-target radiation tube in order to create a conventional x-ray system to be used instead of the synchrotron.

2. EXPERIMENTAL SETUP

Figure 1 shows the circuit diagram of the x-ray generator, which consists of a negative high-voltage power supply, a filament (hot cathode) power supply, and a copper-target x-ray tube. The negative high-voltage is applied to the cathode electrode, and the anode (target) is connected to the ground. In this experiment, the tube voltage was regulated from 12 to 22 kV, and the tube current was regulated by the filament temperature and ranged from 1.0 to 3.0 mA. The exposure time was controlled in order to obtain optimum x-ray intensity.

The experimental setup for performing parallel radiography is shown in Fig. 2. Quasi-monochromatic x-rays are produced using a 10 μm-thick copper filter, and these rays are formed into parallel beams by a polycapillary plate (Fig. 3). The polycapillary is J5022-16 (Hamamatsu Photonics Inc.), and the thickness and the hole diameter of the polycapillary are 1.0 mm and 10 μm, respectively. Radiography was performed by a CR system (Konica Regius 150) utilizing imaging plates.

The distance between the x-ray source and the polycapillary was 1.08 m, and the polycapillary plate was set on the aluminum plate. The distance between the polycapillary and imaging plates was regulated by the height of polymethyl methacrylate (PMMA) spacers of 30 mm in height. At a constant distance between the polycapillary and the imaging plate, the distance between the imaging plate and the chart was regulated by pipe-shaped brass spacers of 30 and 60 mm in height.

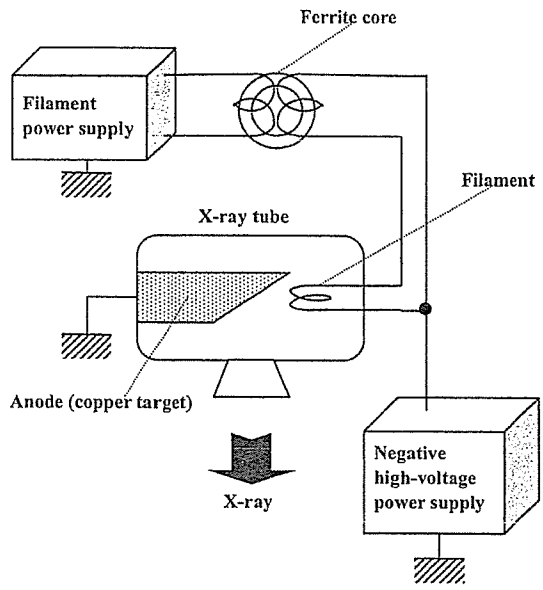

Figure 1: Circuit diagram of the x-ray generator.

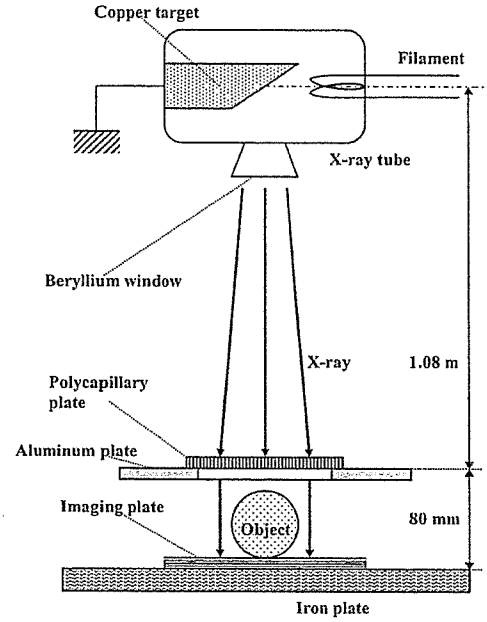

Figure 2: Experimental setup for parallel radiography utilizing a polycapillary plate and a CR system.

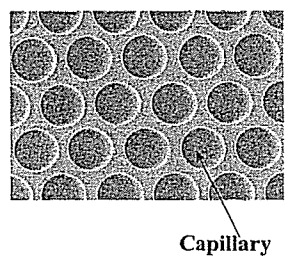

Figure 3: Polycapillary plate.

3. CHARACTERISTICS

3.1 Focal spot

In order to measure images of the x-ray source, we employed a pinhole camera with a hole diameter of 50 μm (Fig. 4). When the tube voltage was increased, the spot intensity increased, and spot dimensions increased slightly and had values of approximately 2.0 × 1.5 mm.

3.2 X-ray spectra

X-ray spectra from the copper-target tube were measured by a transmission-type spectrometer with a lithium fluoride curved crystal 0.5 mm in thickness (Fig. 5). The spectra were taken by the CR system with a wide dynamic range, and relative x-ray intensity was calculated from Dicom digital data. Figure 6 shows measured spectra from the

copper target. When the tube voltage was increased, the bremsstrahlung x-ray intensity increased, and the characteristic x-ray intensity of K_α and K_β lines also increased. Following insertion of the copper filter, the bremsstrahlung x-rays with energies higher than the K-absorption edge were absorbed effectively.

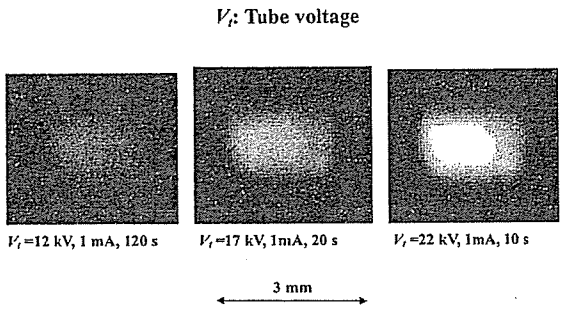

Figure 4: Images of the x-ray source measured by a 50 μm-diameter pinhole with changes in the tube voltage.

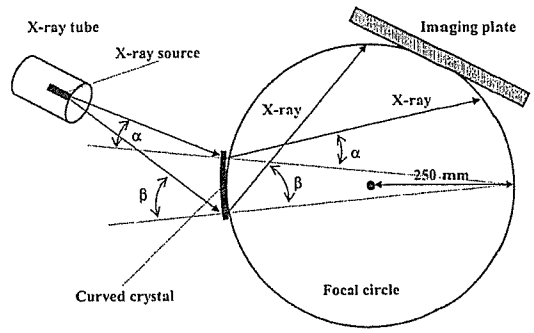

Figure 5: Transmission-type spectrometer with a lithium fluoride curved crystal and an imaging plate.

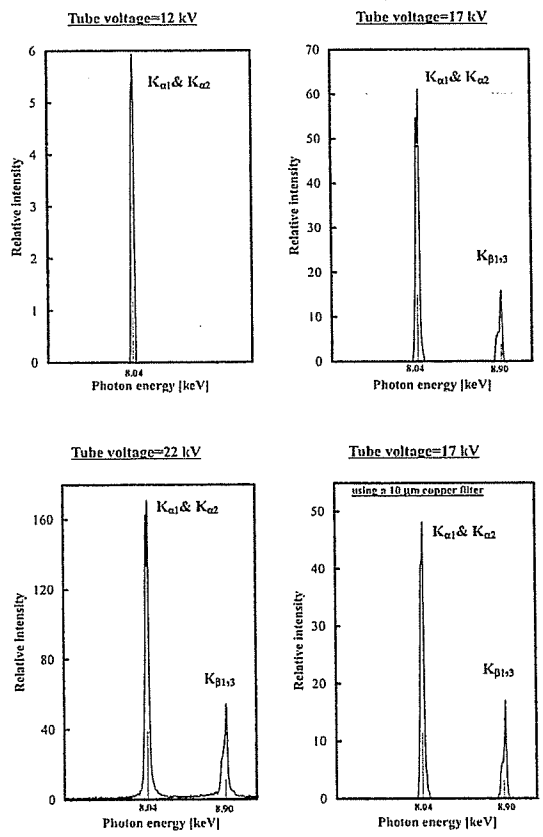

Figure 6: Measured x-ray spectra according to changes in the tube voltage.

4. RADIOGRAPHY

The quasi-monochromatic radiography was performed with a tube voltage of 17 kV using the filter. Figure 7 shows radiography for imaging a polycapillary plate, and the radiograms of the polycapillary are shown in Fig. 8. The center of the black spot in the polycapillary radiogram was mainly imaged by direct transmission beams through capillary holes. As shown in this figure, the spot dimensions increased slightly according to decreases in the PMMA spacer height.

Figure 9 shows the parallel radiography for imaging a test chart, and the polycapillary was set on the aluminum plate. In this radiography, when the spacer height was increased, the image resolution hardly varied, and the image dimensions decreased slightly (Fig. 10). Next, when the height of the brass spacer was decreased, the image resolution hardly varied, and the dimensions again decreased slightly (Figs. 11 and 12).

Figures 13 and 14 show radiography and the radiogram of tungsten wires on a PMMA spacer, respectively. Although the image contrast increased with increases in the wire diameter, a 50 μm-diameter wire could be observed. An angiography of a rabbit heart is shown in Fig. 15; iodine-based microspheres of 20 μm diameter were used, and fine blood vessels of about 50 μm were visible (Fig. 16).

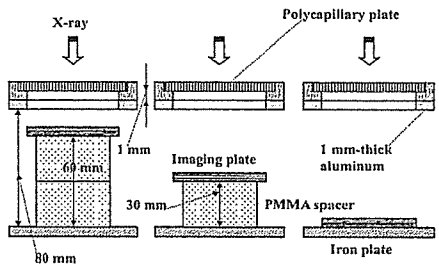

Figure 7: Radiography for imaging a polycapillary plate according to changes in the distance between the polycapillary and imaging plates.

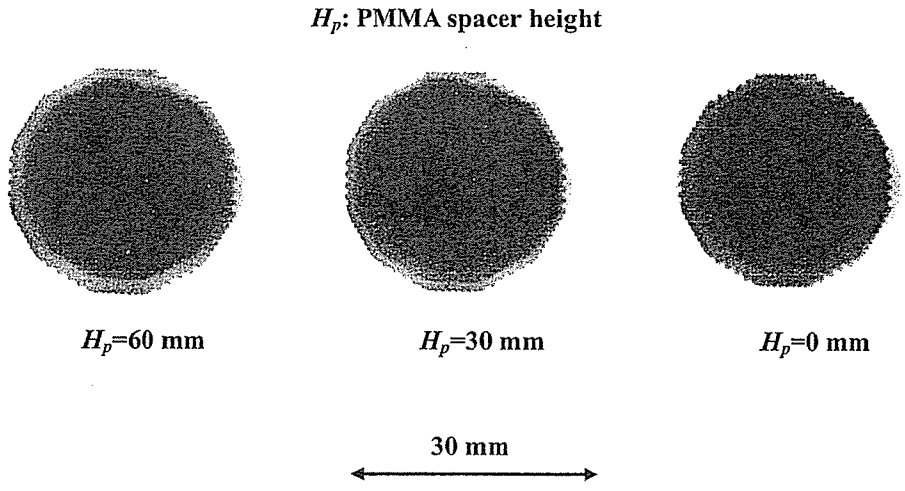

Figure 8: Radiograms of a polycapillary plate according to changes in the PMMA height.

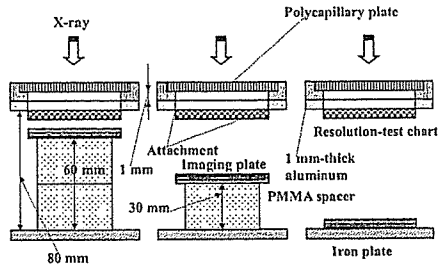

Figure 9: Radiography for imaging a test chart using a polycapillary plate according to the PMMA height.

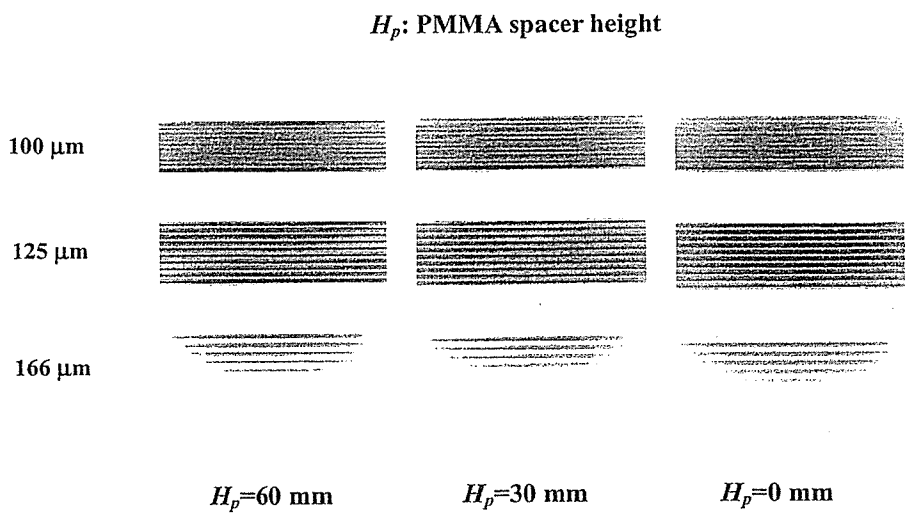

Figure 10: Radiograms of a test chart using a polycapillary plate according to the PMMA height.

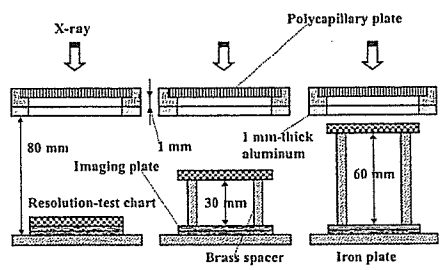

Figure 11: Radiography for imaging a test chart using a polycapillary plate according to the brass spacer height.

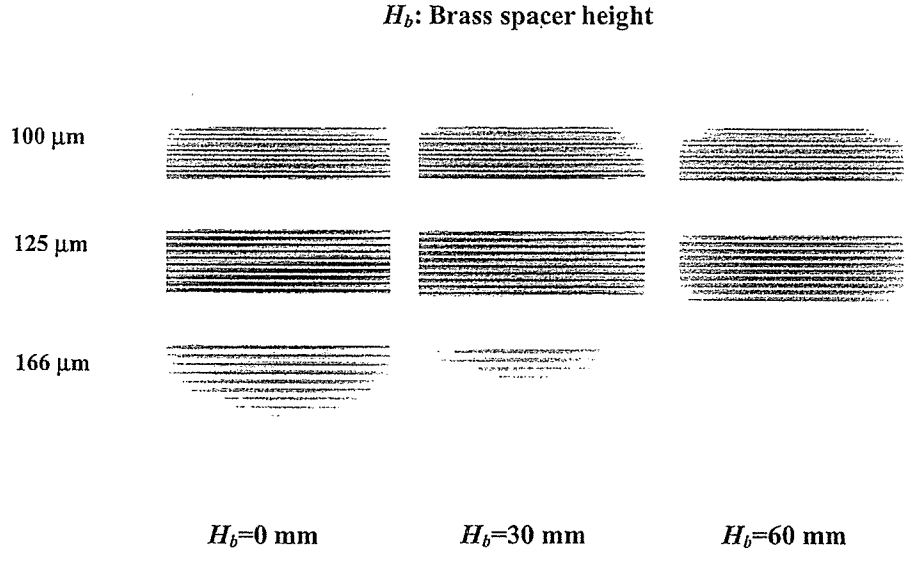

Figure 12: Radiograms of a test chart using the polycapillary according to the brass spacer height.

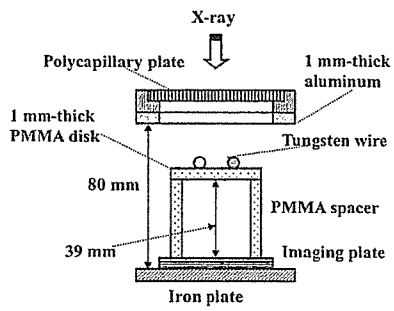

Figure 13: Radiography for imaging tungsten wires using the polycapillary.

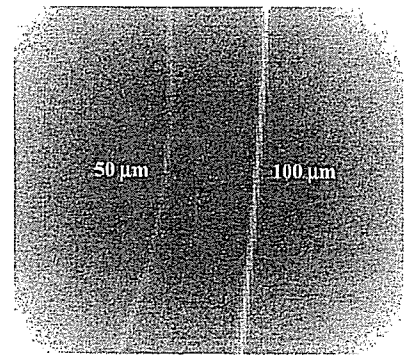

Figure 14: Radiograms of tungsten wires on a PMMA spacer.

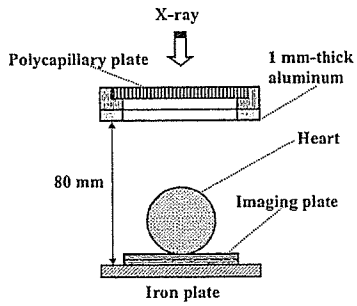

Figure 15: Parallel angiography of a heart extracted from a rabbit using iodine-based microspheres.

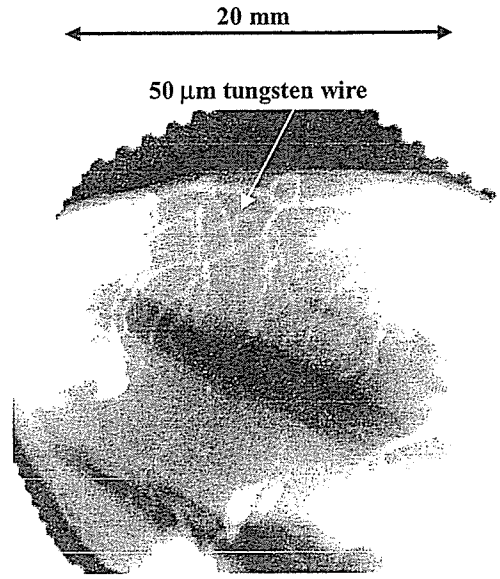

Figure 16: Angiogram of the heart using the polycapillary.

5. DISCUSSION

In this research, we performed parallel radiography achieved with a polycapillary plate in conjunction with quasi-monochromatic x-rays, and obtained slightly higher image resolutions as compared with those obtained without using the plate. Currently, the image resolution of the polycapillary is primarily determined by the diameter of the capillary hole and the thickness, and is improved with decreases in the diameter and increases in the thickness. In cases where the CR system is employed, although the resolution of the CR system is primarily determined by the minimum sampling pitch of 87.5 μm, we could observe 50 μm tungsten wires easily.

The photon energies of the characteristic x-rays are determined by the target element, and the capillary thickness should be increased according to increases in the photon energy because the transmission intensity through capillary glass increases. Subsequently, in order to increase the parallelity for phase imaging, single crystals should be employed after passing through the polycapillary.

Because it is possible to increase the irradiation field by increasing the distance between the x-ray source and the polycapillary, this system can be applied to image a wide variety of objects in various fields, including medical radiography.

ACKNOWLEDGMENTS

This work was supported by Grants-in-Aid for Scientific Research (12670902, 13470154, and 13877114) and Advanced Medical Scientific Research from MECSST, Grants from Keiryo Research Foundation, JST (Test of Fostering Potential), NEDO, and MHLW (HLSRG, RAMT-nano-001, RHGTEFB-genome-005, and RGCD13C-1).

REFERENCES

1. H. Mori, K. Hyodo, E. Tanaka, M.U. Mohammed, A. Yamakawa, Y. Shinozaki, H. Nakazawa, Y. Tanaka, T. Sekka, Y. Iwata, S. Honda, K. Umetani, H. Ueki, T. Yokoyama, K. Tanioka, M. Kubota, H. Hosaka, N. Ishizawa and M. Ando, "Small-vessel radiography in situ with monochromatic synchrotoron radiation," *Radiology*, **201**, pp. 173-177, 1996.

2. T.J. Davis, D. Gao, T.E. Gureyev, A.W. Stevenson and S.W. Wilkims, "Phase-contrast imagimg of weakly absorbing materials using hard x-rays," *Nature*, **373**, pp. 595-597, 1995.

3. A. Momose, T. Takeda, Y. Itai and K. Hirano, "Phase-contrast x-ray computed tomography for observing biological soft tissues," *Nature Medicine*, **2(4)**, pp. 473-475, 1996.

4. A. Ishisaka, H. Ohara and C. Honda, "A new method of analyzing edge effect in phase contrast imaging with incoherent x-rays," *Opt. Rev*, **7**, pp. 566-572, 2000.

5. E. Sato, M. Komatsu, Y. Hayasi, E. Tanaka, H. Mori, T. Kawai, T. Usuki, K. Sato, T. Ichimaru, K. Takayama and H. Ido, "Quasi-monochromatic parallel radiography achieved with a plane-focus x-ray tube," *SPIE*, **4786**, pp. 151-161. 2002.

6. E. Sato, Y. Hayasi, H. Mori, E. Tanaka, K. Takayama, H. Ido, K. Sakamaki and Y. Tamakawa, "Quasi-monochromatic x-ray production from the cerium target," *SPIE*, **4142**, pp. 17-28, 2000.

7. E. Sato, Y. Suzuki, Y. Hayashi, E. Tanaka, H. Mori, T. Kawai, K. Takayama, H. Ido and Y. Tamakawa, "High-intensity quasi-monochromatic x-ray irradiation from the linear plasma target," *SPIE*, **4505**, pp. 154-164, 2001.

8. E. Sato, Y. Hayashi, E. Tanaka, H. Mori, T. Kawai, H. Obara, T. Ichimaru, K. Takayama, H. Ido, T. Usuki, K. Sato and Y. Tamakawa, "Polycapillary radiography using a quasi-x-ray laser generator," *SPIE*, **4508**, pp. 176-187, 2001.

9. E. Sato, Y. Hayasi, E. Tanaka, H. Mori, T. Kawai, T. Usuki, K. Sato, H. Obara, T. Ichimaru, K. Takayama, H. Ido and Y. Tamakawa, "Quasi-monochromatic radiography using a high-intensity quasi-x-ray laser generator," *SPIE*, **4682**, pp. 538-548 2002.

10. E. Sato, Y. Hayasi, E. Tanaka, H. Mori, T. Kawai, K. Takayama and H. Ido, "Irradiation of intense characteristic x-rays from weakly ionized linear plasma," *Proc 3rd Korea-Japan Joint Meeting on Medical Physics, Gyeongju*, pp. 396-399, 2002.

11. E. Sato, Y. Hayasi, R. Germer, E. Tanaka, H. Mori, T. Kawai, H. Obara, T. Ichimaru, K. Takayama and H. Ido, "Intense characteristic x-ray irradiation from weakly ionized linear plasma and applications," *Jpn. J. Med. Imag. Inform. Sci.*, **20**, pp. 148-155. 2003.

12. Q.F. Xiao and S.V. Poturaef, "Polycapillary-based x-ray optics," *Nucl. Instr. Meth. Phys. Res. A*, **347**, pp. 376-383, 1994.

13. A.A. Bzhanmikov, N. Langhoff, J. Schmalz, R. Wedell, V.L. Beloglazov and N.F. Lebedev, "Polycapillary conic collimator for micro-XRF," *SPIE*, **3444**, pp. 430-435, 1998.

14. E. Sato, H. Toriyabe, Y. Hayasi, E. Tanaka, H. Mori, T. Kawai, T. Usuki, K. Sato, H. Obara, T. Ichimaru, K. Takayama, H. Ido and Y. Tamakawa,"Fundamental study on parallel beam radiography using a polycapillary plate," *SPIE*, **4682**, pp. 298-310, 2002.

15. E. Sato , K. Sato and Y. Tamakawa, "Film-less computed radiography system for high-speed Imaging," *Ann. Rep. Iwate Med. Univ. Sch. Lib. Arts and Sci.*, **35**, pp. 13-23, 2000.

Extremely soft x-ray generator and its applications

Eiichi Sato*[a], Fumiko Obata[b], Kiyomi Takahashi[b], Shigehiro Sato[b], Etsuro Tanaka[c], Hidezo Mori[d], Toshiaki Kawai[e], Toshio Ichimaru[f], Kazuyoshi Takayama[g] and Hideaki Ido[h]

[a] Department of Physics, Iwate Medical University, 3-16-1 Honchodori, Morioka 020-0015, Japan
[b] Department of Microbiology, School of Medicine, Iwate Medical University, 19-1 Uchimaru, Morioka 020-8505, Japan
[c] Department of Nutritional Science, Faculty of Applied Bio-science, Tokyo University of Agriculture, 1-1-1 Sakuragaoka, Setagaya-ku 156-8502, Japan
[d] Department of Cardiac Physiology, National Cardiovascular Center Research Institute, 5-7-1 Fujishirodai, Suita, Osaka 565-8565 Japan
[e] Electron Tube Division #2, Hamamatsu Photonics Inc., 314-5 Shimokanzo, Toyooka Village, Iwata-gun 438-0193, Japan
[f] Department of Radiological Technology, School of Health Sciences, Hirosaki University, 66-1 Honcho, Hirosaki 036-8564, Japan
[g] Shock Wave Research Center, Institute of Fluid Science, Tohoku University, 2-1-1 Katahira, Sendai 980-8577, Japan,
[h] Department of Applied Physics and Informatics, Faculty of Engineering, Tohoku Gakuin University, 1-13-1 Chuo, Tagajo 985-8537, Japan

ABSTRACT

The development of an extremely soft x-ray generator with a tungsten-target tube and its applications to radiography and disinfection are described. This generator consists of a high-voltage power supply, a filament power supply, and an x-ray tube. Negative high voltages are applied to the cathode electrode in the x-ray tube, and the tube voltage and current are regulated by the input of a transformer and the filament voltage, respectively. The x-ray tube is a glass-enclosed double-focus diode with a tungsten target and a 0.2 mm-thick beryllium window. The maximum tube voltage and electric power were 60 kV and 400 W, respectively. The focal-spot sizes were 4×4 (large) and 1×1 mm (small), respectively. Extremely soft radiography was performed with a computed radiography system, and we observed fine blood vessels of about 100 μm with high contrasts. Using this generator, we performed the disinfection achieved with extremely soft x rays.

Keywords: extremely soft x-ray, thin beryllium window, soft x-ray disinfection, soft radiography

1. INTRODUCTION

Synchrotrons generate high-dose-rate bremsstrahlung x rays with wide photon energy latitudes, and monochromatic x-ray beams have been produced using single crystals. These rays have been employed to perform K-edge angiography[1-3] and phase imaging.[4-6] However, it is difficult to increase the irradiation field, due to the parallel beam, or to obtain sufficient machine times for various research projects, including medical applications.

Conventional medical x-ray generators produce both bremsstrahlung and characteristic x rays, and quasi-monochromatic x rays have been produced using K-edge filters. In contrast, flash x-ray generators utilize cold-cathode tubes, and the generators[7-13] with photon energies of lower than 150 keV can be employed to perform biomedical radiography. In order to produce monochromatic x rays, plasma flash x-ray generators[14-18] are useful, since quite intense and sharp characteristic x rays such as lasers have been produced from weakly ionized linear plasmas.

In order to produce monochromatic parallel beams using a hot-cathode x-ray tube in conjunction with the crystals, high-dose-rate bremsstrahlung x rays are needed, and the x-ray photon energy is selected by Bragg's angle. Therefore,

X-Ray Sources and Optics, edited by C. A. MacDonald, A. T. Macrander, T. Ishikawa, C. Morawe, J. L. Wood, Proc. of SPIE Vol. 5537 (SPIE, Bellingham, WA, 2004) · 0277-786X/04/$15 · doi: 10.1117/12.560551

the thickness of the x-ray window of the tube should be decreased as much as possible so as to increase the x-ray dose rate and to produce soft bremsstrahlung x rays. In addition, soft x rays are useful to image soft-tissue objects, including biomedical objects, and the rays may be used to perform disinfection of various fungi, including anthrax, because the x rays are absorbed easily by fungi.
In the present research, we developed an extremely soft x-ray generator with a tungsten-target tube, and used it to perform preliminary studies on extremely soft radiography and disinfection.

2. GENERATOR

Figure 1 shows the block diagram of the x-ray generator, which consists of a high-voltage power supply (Fig. 2), an x-ray tube unit (Fig. 3), and a filament power supply. The negative high voltage is applied to the cathode electrode, and the anode (target) is connected to the ground potential. The x-ray tube is a glass-enclosed diode with a tungsten target and a 0.2 mm-thick beryllium window. In this experiment, the peak tube voltage was regulated from 10 to 15 kV using an auto transformer, and the peak tube current was regulated within 15 mA by the filament voltage (temperature). The exposure time is controlled in order to obtain optimum x-ray intensity, and the x-ray tube is a double-focus type with focal-spot dimensions of approximately 4×4 (large spot) and 1×1 mm (small spot), respectively.

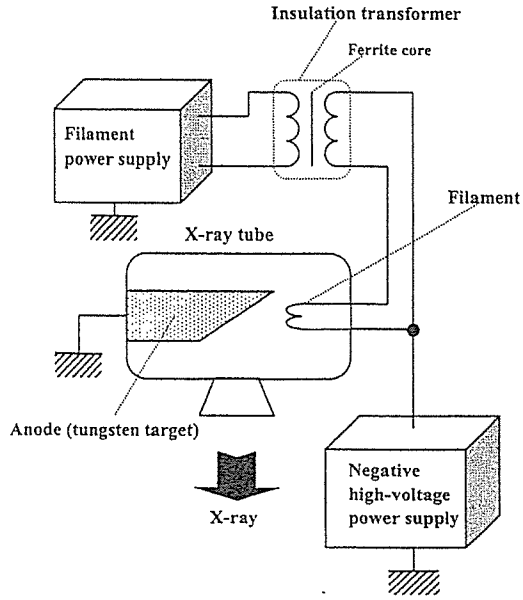

Fig. 1. Block diagram of extremely soft x-ray generator.

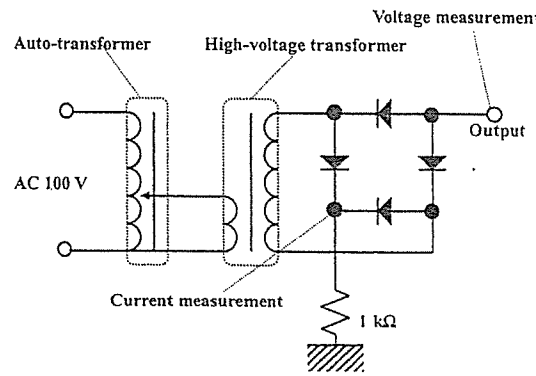

Fig. 2. Circuit diagram of high voltage power supply.

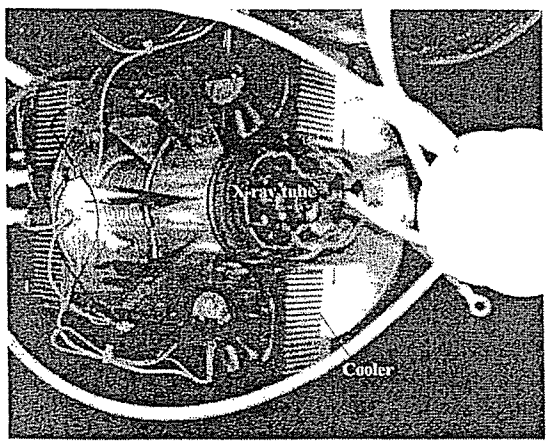

Fig. 3. X-ray tube unit with coolers.